

OMAE2014-24647

MODEL TESTING OF FISH FARMS FOR VALIDATION OF ANALYSIS PROGRAMS

Are Johan Berstad

Dr.Ing. Aquastructures
Oslo, Norway

Email: are.berstad@aquastrucures.no

Line Fludal Heimstad

M.Sc. Aquastructures
Trondheim, Norway

Email: line@aquastrucures.no

Jørgen Walaunet

M.Sc. Aquastructures
Rørvik, Norway

Email: jw@aquastrucures.no

ABSTRACT

This paper presents a case study where results from numerical analysis have been compared to model experiments, performed on a 1/16 scale model. The tested model is a circular cage system with a polyethylene cage. The system is tested both in waves and current.

Numerical analysis to document the structural integrity of the fish farms are now a requirement. The state of the art analysis tool used in the aquaculture industry is AquaSim [1].

Results from model experiments are compared to numerical analysis carried out in AquaSim. Uncertainties in the model experiments are investigated and discussed. The differences between the experimental and numerical results are in the same range as the uncertainties.

NOMENCLATURE

A Cross sectional area
 D_{rope} Diameter of mooring line
E Young's modulus
 H_{net} Depth of net
I 2^{nd} area moment of inertia
 L_w Weight of bottom weight
O Circumference of floater
R Force
r Displacement
 \bar{r} Prediction for r
Sn Solidity ratio of the net
T Wave period
 W_b Weight of sinker tube

$U(\alpha)$ Angle of incoming current

INTRODUCTION

In 2009, the Norwegian standard NS 9415 [2] was revised and in 2011 corresponding regulations were enforced. This largely increased the number of analysis being carried out. At present all fish farms in Norway is required to document structural integrity by analysis.

Fish farms deviate from other marine structures normally tested in model basins. This introduces extra challenges both for the model experiments itself, and the comparison between model experiment and numerical analysis. Among the challenges are:

Scaling dimensions

Size of measurement equipment and their influence on measured results

Measuring and reporting all input parameters, as an example how are ropes preloaded

Basic equilibrium and reporting

This paper presents a case study where results from numerical analysis have been compared to results from model experiments, carried out for a 1/16 scale model. The geometry of the model is one of the most typical fish farm geometries used in Norway and is shown in Fig. 1. This is a circular cage system with polyethylene cage.

The sensitivity of the input parameters are investigated. This forms a basis for the design criteria.

The paper goes on to conclude on how this should be treated in current design criteria and suggestions for useful testing.



FIGURE 1. TYPICAL NORWEGIAN FISH FARM [3]

THEORETICAL BASIS FOR THE ANALYSIS PROGRAM AQUASIM

The AquaSim program is based on the finite element method. It utilizes beam and shell elements with rotational DOF's, as well as membrane elements and truss elements with no rotational stiffness. Geometric non-linearities are accounted for in all element types, such that the program handles large structural deformations. The program is based on time domain simulation where it is iterated to equilibrium at each time instant. Both static and dynamic time domain simulation may be carried out. Features such as buoys, weights, hinges and springs are included in the program.

The basic idea of the FE analysis program is to establish equilibrium between external loads acting on the structure at a given time instant and internal reaction forces.

$$\sum F = R_{ext} + R_{int} = 0 \quad (1)$$

where R_{ext} is the total of the external static forces, acting on the structure at a given time instant, and R_{int} is the internal forces. The structure is discretized to a finite number of degrees of freedom DOF's. Equation 1 is then discretized as:

$$F^{idof} = R_{ext}^{idof} + R_{int}^{idof} = 0, idof = 1, N_{dof} \quad (2)$$

where N_{dof} is the discrete number of DOF's the structure has been discretized into. The current element program deals with strongly non-linear behaviour both in loads and structural response. In order to establish equilibrium, the tangential stiffness method is used. External loads are incremented to find the state of equilibrium. Having established equilibrium in time step $i-1$, the condition for displacement r , step i , is predicted as:

$$\Delta R_{ext}^i(r_{i-1}) + R_{int}^{i-1}(r_{i-1}) = K_t^{i-1} \Delta r \quad (3)$$

where K_t^{i-1} is the tangential stiffness matrix at configuration $i-1$. The external load is calculated based on the configuration of the structure at $i-1$. This gives a prediction for a new set of displacements ($j=1$). Based on Eqn. 3, a prediction for the total displacement $r(j=1)$, is found as:

$$\bar{r}_{j=1} = r_{i-1} + \Delta r \quad (4)$$

Based on this estimate for new displacements, both external and internal forces are derived based on the new structural geometry and the residual force, ΔR , is put into the equation of equilibrium as follows:

$$\Delta R(\bar{r}_j) = R_{ext}^i(\bar{r}_j) + R_{int}^i(\bar{r}_j) = K_t^i \Delta r \quad (5)$$

Note that both the external and the internal forces will vary for each iteration due to the strongly hydro-elastic nature of the fluid structure interaction. Equation 5 is solved for the displacement Δr . Incrementing j with one, the total displacement is now updated as:

$$\bar{r}_j = \bar{r}_{j-1} + \Delta r \quad (6)$$

Now if Δr found from Eqn. 5 is larger than the tolerated error in the displacements, Eqn. 4 is updated ($j=j+1$) and Eqn. 5 is solved based on the new prediction for displacements, this is repeated until Δr is smaller than a tolerated error, then:

$$r_i = \bar{r}_j \quad (7)$$

i is increased with one, and Eqn. 4 is carried out for the new load increment.

At the default configuration, the program works as this: Static analysis is used to establish static equilibrium including buoyancy. Secondly, current loads are applied then wind and wave loads are added (still static analysis). Then dynamic analysis commences. Waves are introduced with the first wave used to build up the wave amplitude. Both regular waves and irregular waves may be simulated. Waves are assumed to be sufficiently described by linear wave theory. Inertia and damping are accounted for in the wave analysis, meaning that mass and damping are accounted for in the equations of equilibrium. The Newmark-Beta scheme is applied for the dynamic time domain simulation [4]. Note that the above equations imply using the Euler angles for rotations. This is just a simplification for easy typing. For rotational DOF's AquaSim uses a tensor formulation for the rotations as outlined in [5] which must be applied to handle 3D rotations in an appropriate manner.

Wave loads may be derived using the Morrison formulae [6] or using diffraction theory. The diffraction theory used in AquaSim is a form of "strip theory" [7], but in this case hull forces are derived by direct pressure integration over the mean hull surface. Diffraction loads may be applied to beams or truss elements. Linearized values for diffraction, added mass and damping are derived for the elements mean wetted position. For irregular waves, linearized added mass and damping for the characteristic period in the wave spectrum are used in the calculations. Wave interaction between separate components is not accounted for. For further description on how this is handled see [8,9]. For components that are small compared to the wave length the Morrison equation [6] is normally applied whereas for larger components, such as barges, diffraction theory is applicable [7].

When the Morrison formulae is used, the cross flow principle is applied for beams and truss elements (see. e.g. [10]). The drag load term of this equation is quadratic with respect to the relative velocity between the undisturbed fluid and the structure, both the mass of the structure as well as added mass in the cross sectional plane are accounted for. Due to the large deflections occurring, the added mass is non-linear.

For the membrane elements, representing mesh used in fish nets as shown in Fig. 2, the Morrison equation is used as basis for the load formulations, with some modifications outlined in [11].



FIGURE 2. TYPICAL NET USED IN A FISH FARM

Basically each twine is considered a cylinder. In [11] flow through a mesh is compared to flow around a cylinder. The flow velocity must increase passing through a net since the net leads to smaller area for the water to flow through. This can be accounted for by increasing the drag coefficient. In [11] the following drag coefficient $C_{d_{mem}}$ is introduced as:

$$C_{d_{mem}} = C_{d_{cyl}} \frac{1}{(1 - \frac{d}{L})^3} \quad (8)$$

Where $C_{d_{cyl}}$ is the drag coefficient relevant for one single twine (baseline in Fig. 3) and $L = L_y = L_z$ as shown in Fig. 3.

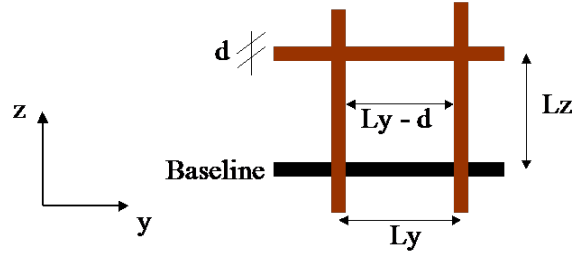


FIGURE 3. MATHEMATICAL DESCRIPTION OF TWINE

Note that the formulation for $C_{d_{cyl}}$ given herein differs from the formulation found in e.g. [12–14] which originates back to [15].

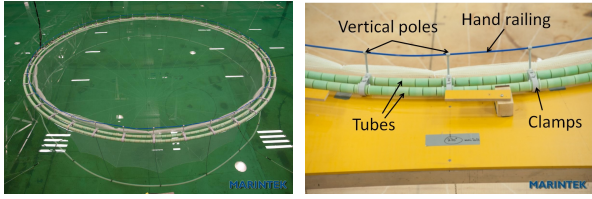
As further described in [11] the drag coefficient will also depend on the angle of the incident flow relative to the mesh giving much less drag for flow parallel to the net. Current reduction from upstream betting is applied according to [16]. Alternative formulations are given in [12, 17]. This will be considered for introduction to AquaSim.

AquaSim has undertaken a versatile verification scheme: Analysis has been carried out on a wide range of computational cases where results have been compared to handbook formula or other programs, see [18]. Tank testing has been carried out and compared to analysis, see [19]. The program has been compared to accidents where the capsize origins were known [20,21]. In addition experience have been obtained during several years where the program has been the most used program for calculation of the structural integrity of fish farm systems in Norway. These systems in general consist of moorings, structure and nets responding to wave and current in a strongly hydro-elastic manner. The program is also used for a wide range of offshore applications such as towing for seismic operations [22], operations and installations offshore, mooring analysis of offshore units and structural and mooring analysis of equipment for renewable equipment offshore [23].

MODEL TEST CASE

The model experiments have been carried out at the Ocean Basin Laboratory at MARINTEK. A 1/16 scale model of a polyethylene fish farm have been exposed to current, as well as both regular and irregular waves. The main particulars of the model set-up are presented in [24]. The model is shown in Fig. 4(a). Information presented in this paper, which is not presented in [24], has been found from dialogue with the author of this report.

Figure 4(b) shows details of the tested model. A floater with two tubes ensuring buoyancy, clamps, poles and hand railing. The test cases in the wave analysis, from the model experiments, are listed in Tab. 1.



(a) CAGE SYSTEM WITH (b) FLOATER, TESTED MODEL FLOATER AND NET

FIGURE 4. Experimental model from [24]

TABLE 1. TEST CASES WAVE ANALYSIS

Test case	Current [m/s]	H [m]	T [s]
3010	0.5	0	0
3150	0	2.5	6
3160	0	2.5	8
3170	0.5	2.5	6
3180	0.5	2.5	8

NUMERICAL ANALYSIS OF THE MODEL EXPERIMENT

This section compares numerical results, obtained through AquaSim, to the results from the model experiments. Loads are compared at four locations, two mooring lines and two bridles, located upstream as seen in Fig. 5. This numerical model have been established in the full scale coordinate system. The mooring lines are numbered from 1-8. Positive current at 0 degrees flows parallel with the x- axis. The bridles are attached to the floater at clamp 2 and 7 from the x- axis corresponding to 18 and 63 degrees [Deg] about the z- axis in a system symmetric about both the x- and the y- axis.

All parameters applied in the numerical model is given in Appendix 1. It should be noted that of the 75 input parameters used in this analysis, 33 parameters have been found from [24] or by extra information from MARINTEK, and 42 input parameters have been estimated.

Pretension

In order to compare numerical results and experiments one should know the pretension of the system, i.e. the stresses in the system without current and waves. The report and result files, from the model experiments, did not present separate results for the pretension of the system. However in test case 3150 and 3160 (see Tab. 1) the first part of the time series is without current and waves. These are used as basis of the pretension.

In AquaSim pretension is introduced to components. The normal analysis approach is to calculate static equilibrium and then find the status of pretension. This analysis model is called

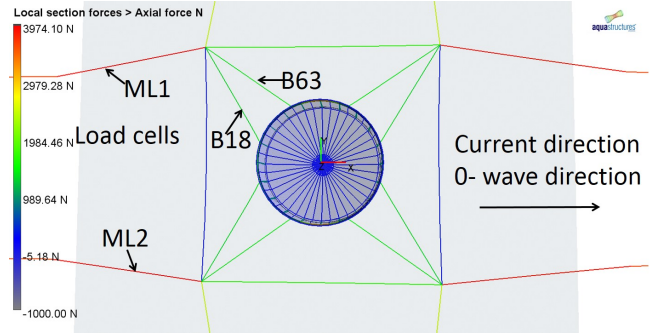


FIGURE 5. LINE NUMBERS IN THE NUMERICAL MODEL

M0 and results in terms of line tension is shown in Fig. 6.

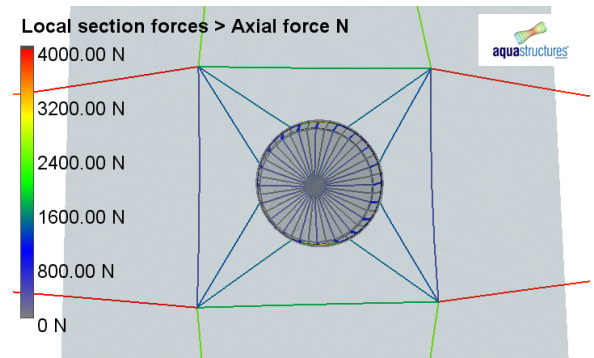


FIGURE 6. MODEL M0, PRETENSION DUE TO GEOMETRY

The tension in the analysis model, M0, is compared to experiment at the four positions shown in Fig. 5. Results are compared in Fig. 7.

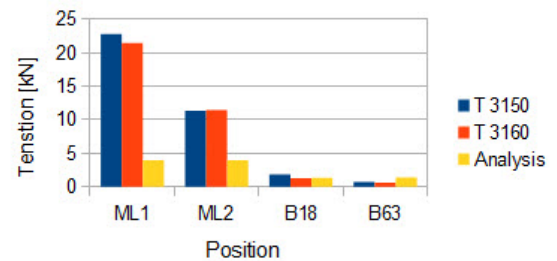


FIGURE 7. NUMERICAL MODEL M0 COMPARED TO EXPERIMENTS. PRETENSION

As seen from Fig. 7 there is a good correspondence in the pretension for the bridles, while the mooring lines have more

pretension in the model experiment than in the numerical model M0.

Note that the results from the model experiment, for the mooring line at position ML1 (see Fig. 5), shows approximately twice the tension as the tension in ML2. If the model had been symmetrical the pretension of the lines should have been equal.

A model M0.5 is established and shown in Fig. 8. Here additional pretension have been applied to all mooring lines. This to get the numerical model more equal to the model used in the experiments. Note that there are no reported data of the pretension in the lines transverse to the current direction. This represents an uncertainty.

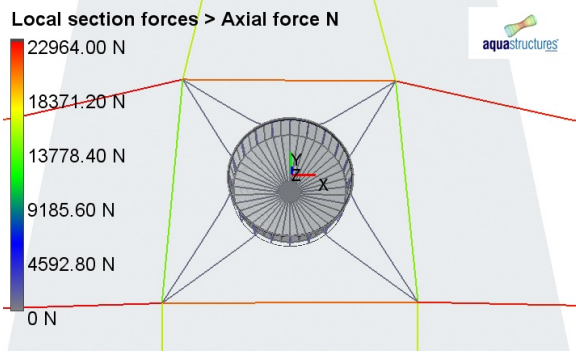


FIGURE 8. INTERMEDIATE MODEL, M0.5

As seen from Fig. 8 the line tension in ML1 is the same as in the model experiment. Due to symmetry the tension in the mooring line ML2 is the same as ML1. A new model M1 is therefore established where the pretension in ML2 is decreased. The line tension is seen in Fig. 9.

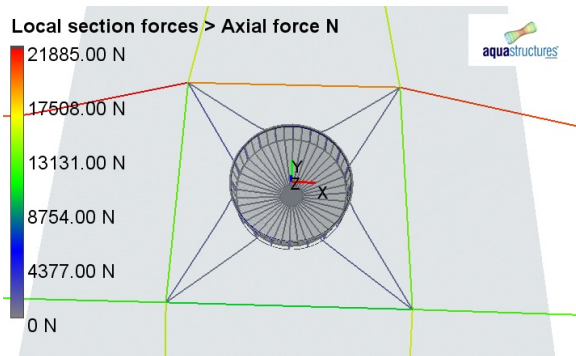


FIGURE 9. AQUASIM MODEL M1

Figure 10 shows line tension in the numerical model M1. As seen from this figure there is a good correspondence in line

tension for model M1. This numerical model is therefore used for further study.

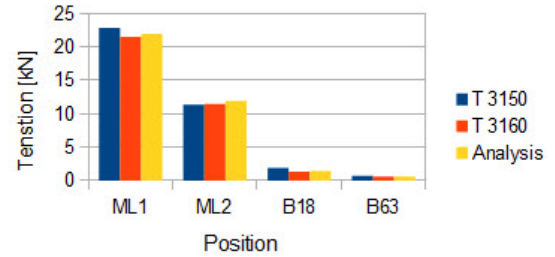


FIGURE 10. M1 NUMERICAL MODEL COMPARED TO EXPERIMENTS. PRETENSION

Current

Numerical analysis is carried out for test 3010 (see Tab. 1). This is the system exposed to 0.5 [m/s] current along the x- axis and no waves.

Comparison between numerical and experimental results are shown in Fig. 11. As seen from this figure there is a good correspondence in forces for mooring line ML1 and ML2. For the bridles the combined tension in the two bridles, B1863, shows good correspondence with the analysis. The numerical results shows a more even distribution of forces between the bridles. Most probable this is due to difference in the pretension condition.

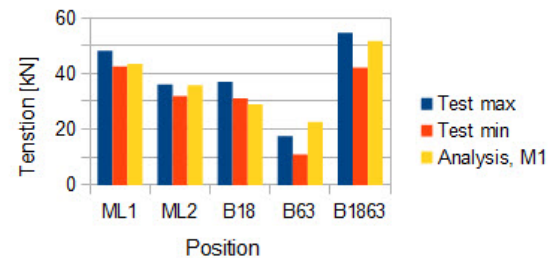


FIGURE 11. RESPONSE, M1, CURRENT 0.5 [M/S]

Waves

Figure 12 presents forces obtained through the model experiments at the four locations shown in Fig. 5.

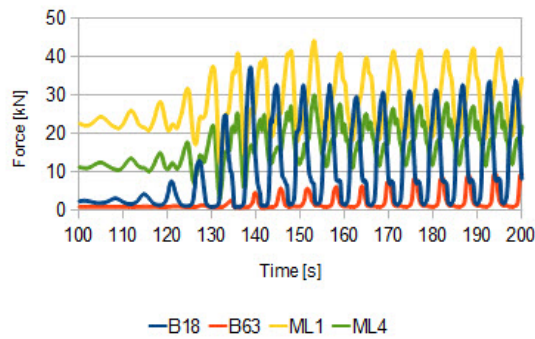


FIGURE 12. EXCERPT OF MEASURED FORCES TEST 3150

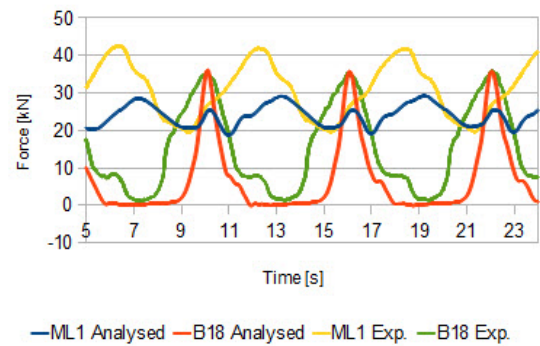


FIGURE 14. EXCERPT FROM ANALYSIS AND MEASUREMENT. TEST CASE 3150

Figure 13 presents results, from the model experiment (denoted Exp.) compared to results from the numerical analysis, for test 3150. As seen from the figure the forces in the bridles correspond well. Forces in the mooring lines are lower in the numerical analysis compared to the model experiment.

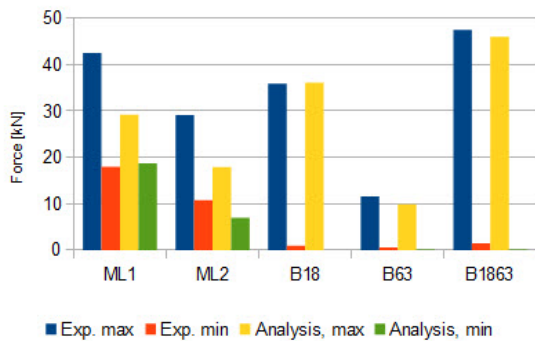


FIGURE 13. TEST 3150 COMPARED TO ANALYSIS

Figure 14 shows an excerpt of the time series from the numerical results compared to experiment for bridle B18 and mooring line ML1. As seen from the figure the results for the bridle B18 is highly nonlinear both in the analysis and the testing. An effect typical for fish farms systems is observed. That is a line varying between being unloaded and slack to taking high peak loads.

Figure 15 shows comparison between experimental and numerical results for test case 3160. As seen from this figure there is a good correspondence in forces. The largest difference between the results is for line B63. This mooring line have however a strong uncertainty in the initial conditions as the line is slack at the pretension condition.

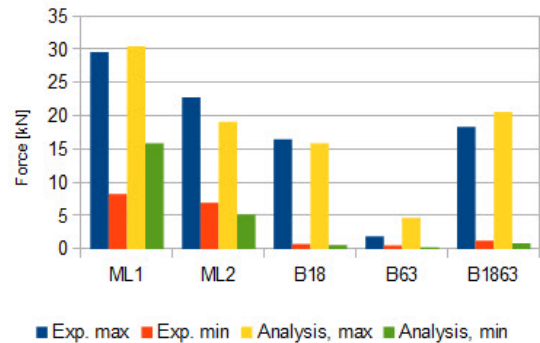


FIGURE 15. TEST 3160 COMPARED TO ANALYSIS

Figure 16 shows an excerpt of the test time series and the analysis time series. As seen the results compare very well.

Waves And Current Combined

Test 3170 is a case which is close to a normal design criteria case according to the standard for fish farm units, NS 9415 [2]. Figure 17 shows test case 3170 compared to numerical analysis. As seen from the figure results compare well to analysis.

Figure 18 shows the analysis for test case 3170. Analysis has been carried out for a total of 8 wave cycles. From the figure the build up of drift is seen. This is caused by the combination of wave and current forces, which gives a mean force in the current direction that is higher than the mean force caused by current alone. This originates from the non-linear drag term in the Morrison equation.

Figure 19 shows a more detailed comparison of analysis and measurements. As seen results compare well in this case with respect to amplitudes, and the phase-shift between forces in the mooring lines relative to the bridles in the measurements.

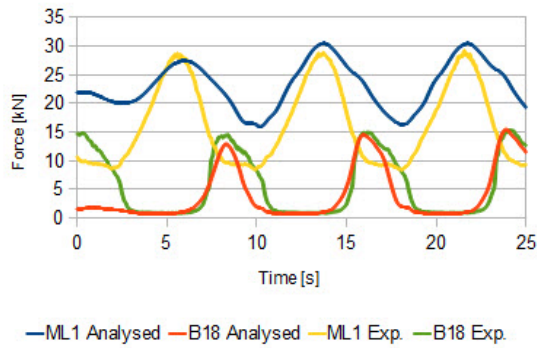


FIGURE 16. EXCERPT FROM ANALYSIS AND MEASUREMENT. TEST CASE 3160

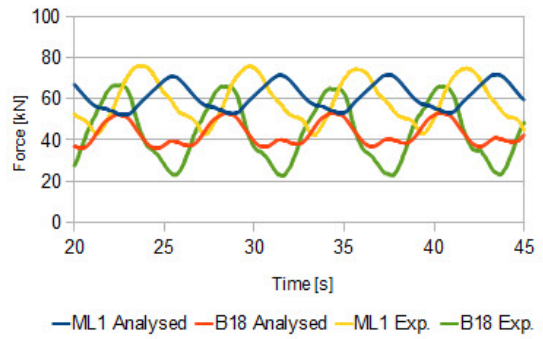


FIGURE 19. EXCERPT FROM ANALYSIS AND MEASUREMENT TEST CASE 3170

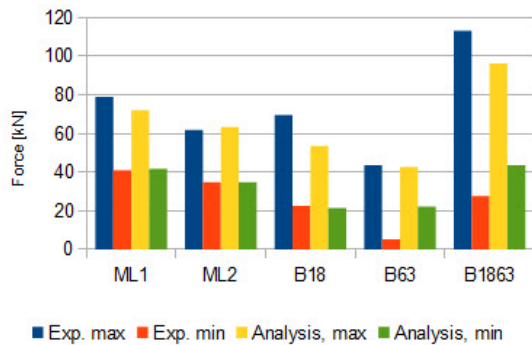


FIGURE 17. TEST 3170 COMPARED TO ANALYSIS

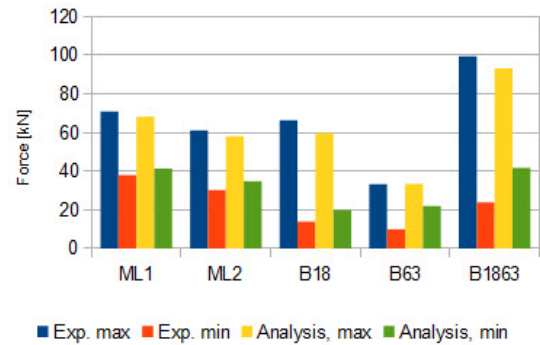


FIGURE 20. TEST 3180 COMPARED TO ANALYSIS

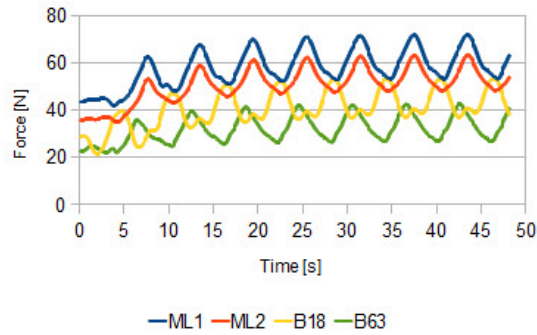


FIGURE 18. ANALYSIS RESULTS FOR TEST 3170

Results from test case 3180 show the same trend as for 3170. As seen from Fig. 20 there is less discrepancy between measurements and analysis for this case than for case 3170.

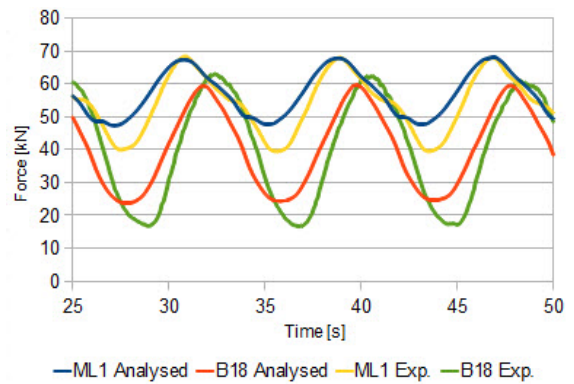


FIGURE 21. EXCERPT FROM ANALYSIS AND MEASUREMENT TEST CASE 3180

SENSITIVITY ANALYSIS

A sensitivity analysis has been performed in order to get a view on what effect a change in different parameters will have on the overall results. In this sensitivity analysis one parameter, at time, has been varied a certain percentage, while holding all other parameters fixed. The nominal values will be the dimensions given in [24], and the numerical model in AquaSim will be exposed to current in the range of $U = 0 - 0.5$ [m/s]. The parameters varied in the sensitivity analysis are listed in Tab. 2. The axial force from the upstream mooring line, denoted "ML1" in Fig. 5, has been used as basis in the sensitivity analysis. It is a bit of a challenge to carry out a sensitivity analysis on parameters of a different nature. Typically 20% variation in a tube diameter is a much less propable variation than 20% variation in rope stiffness. In this analysis it is however made a "brute force" approach and all parameters have been varied 20% from its mean position. This should however be subject to a refined sensitivity analysis.

TABLE 2. PARAMETERS VARIED IN THE SENSITIVITY ANALYSIS

Parameter	Nominal value	Variation	N_{var}
Sn	0.26	$\pm 20\%$	2
W_b	25 [kg/m]	$\pm 20\%$	2
L_w	200 kg	$\pm 20\%$	2
D_{rope}	56 [mm]	$\pm 20\%$	2
E_{rope}	2.44E+10 [N/m ²]	$\pm 20\%$	2
O	157 [m]	$\pm 20\%$	2
H_{net}	25 [m]	$\pm 20\%$	2
$U(\alpha)$	0 [deg]	$\pm 20\%$	2

The total uncertainty related to the parameters listed in Tab. 2 is found by varying these parameters individually. The uncertainty from one parameter at each current velocity, U , is found by:

$$\Delta F_i = \frac{1}{N_{var}} \sum_{j=1}^{N_{var}} |F_0 - F_j| \quad (9)$$

Where F_0 is the nominal force, F_j is the force from the run with variation and N_{var} is the number of variation given in Tab. 2. The relative uncertainty associated with each parameter listed in Tab. 2 and presented in Fig. 22 are found from the following expression:

$$F_{rel} = \frac{\Delta F_i}{F_0} \quad (10)$$

The total uncertainty is then found by taking the sum of each individual uncertainty as:

$$\Delta F = \left(\sum_i (\Delta F_i)^2 \right)^{1/2} \quad (11)$$

As seen from Fig 22 the relative uncertainty related to the solidity ratio, Sn , is the dominant part of error in the low velocity range. However as the current velocity increase the relative uncertainty flattens out and shows the tendency to decrease as the net deformation becomes more pronounced.

The relative uncertainty related to the sinker tube, i.e. W_b shows the opposite trend, where the uncertainties increase with increasing current velocity.

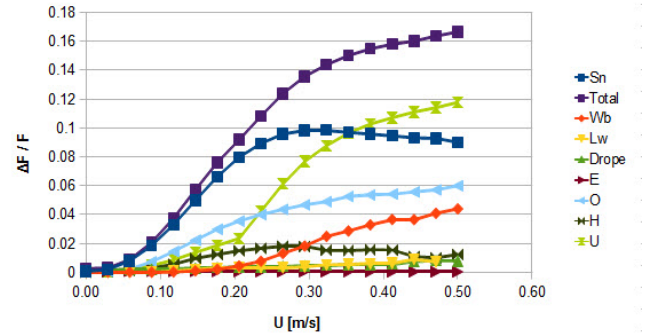


FIGURE 22. RELATIVE UNCERTAINTY

The nominal values along with the total error bounds are presented in Fig. 23.

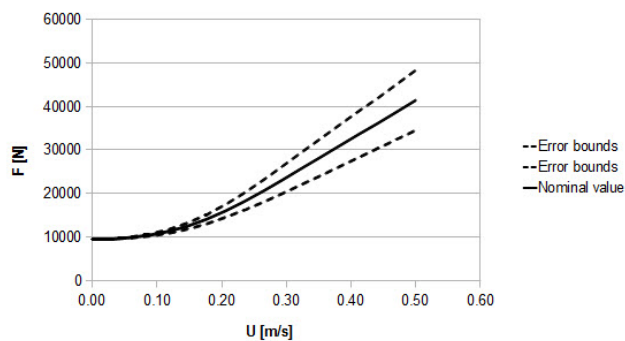


FIGURE 23. TOTAL UNCERTAINTY

DISCUSSION AND CONCLUSION

In the experiment only 33 out of 75 input parameters (from [24]) was documented. The remaining 42 parameters, used in the numerical analysis, are estimated based on previous experience. This limits the accuracy level of the numerical results.

The pretension conditions, of the mooring lines in the model experiment, shows a skewed distribution, although the model is symmetric. The pretension of mooring line ML1 was twice the pretension of mooring line ML2. There is no data for the pretension of the remaining mooring lines and the pretension in these lines is an uncertainty.

The model experiments carried out at MARINTEK [24] had a much broader scope than to be used in this numerical analysis. It can hence not be expected that all the reported data from the model experiments address the necessary input to this numerical analysis. This illustrates the trade-off between model experiments with small and large scope, and also the need for a broad range of model experiments and an good information flow. This to calibrate the software tools such that the fish farm facilities meets the design criteria.

The software tool AquaSim is able to accurately calculate non-linear responses in mooring lines, where the loads in the mooring lines experiences snap loads, i.e. goes from slack to tense.

In general the numerical results shows good correspondence with the results from the model experiment. The numerical results are within the accuracy limited by the scope of measurements. This includes the numerical analysis with current and waves, and the numerical analysis with current and waves combined.

The difference, between the numerical and experimental results, are highest for the analysis with the steepest waves. This can be an indication that some of the largest uncertainties in the analysis may be the inertia of the system. This caused by a wide range of mass contributors, such as added mass effect of fluid in-

side the net, and the additional mass of the measurement equipment. It would be of large interest to perform further study the effective added mass of fluid inside a net.

The sensitivity analysis shows that a 20% change of the input parameters leads to about 20% change in results. The sensitivity analysis should be combined with an assessment of probability for parameter variation to obtain a more refined sensitivity analysis.

ACKNOWLEDGMENT

The work has been funded by Aquastructures AS and the Norwegian research council, NFR. Their support is acknowledged.

REFERENCES

- [1] Berstad, A. J., Report No. 2006-Fo06. Aquasim, the aquastructuresimulator, theoretical formulation of structure and load modelling. Tech. rep., Aquastructures. www.aquastructures.no.
- [2] Marine fish farms, Requirements for site survey risk, analysis, design, dimensioning, production, installation and operation, 2009. *NS 9415*.
- [3] <http://www.atelierdeschefs.fr/blog/pourquoi-latelier-des-chefs-recommande-les-produits-de-la-mer-de-norvege>.
- [4] Langen, I., and Sigbjørnsson, R., 1979. *Dynamisk analyse av marine konstruksjoner*. TAPIR forlag, Trondheim Norway.
- [5] Eggen, T., 2000. "Buckling and geometrical nonlinear beam-type analyses of timber structures". PhD thesis, NTNU.
- [6] Morison, J., O'Brien, M., Johnson, J., and Schaaf, S., 1950. "The force exerted by surface waves on piles". *Journal of Petroleum Technology*, **Volume 2**(Number 5), May, pp. 149–154.
- [7] Salvesen, N., Tuck, E., and Faltinsen, O., 1971. *Ship motions and sea loads*. Det norske Veritas, Oslo.
- [8] Fahti, D., 1996. Veres version 2.0 - user's manual. Tech. rep., MARINTEK, Marintek 7034 Trondheim Norway.
- [9] Berstad, A. J., 2013. On the analysis of moored large mass floating objects and how to carry out such analysis with aquasim, report no. 2174-1, rev. no. 02. Tech. rep., Aquastructures AS 2013.
- [10] Faltinsen, O., 1990. *Sea loads on ships and offshore structures*. Cambridge University Press.
- [11] Berstad, A. J., Walaunet, J., and Heimstad, L. F., 2012. "Loads from currents and waves on net structures". *27th International Conference on Offshore Mechanics and Arctic Engineering*, June 15-20. Rio, Brazil.
- [12] Blevins, R. D., 1984. *Applied fluid dynamics handbook*. Malabar, Fla. : Krieger Publ. Co.,.

- [13] Balash, C., Colbourne, B., Bose, N., and Raman-Nair, W., 2009. "Aquaculture net drag force and added mass". *Aquacultural Engineering*, **41**(1), pp. 14 – 21.
- [14] Molin, B., 2011. "Hydrodynamic modeling of perforated structures". *Applied Ocean Research*, **33**(1), pp. 1 – 11.
- [15] Darcy, H. *Les Fontaines Publiques de la Ville de Dijon*. Victor Dalmont, Libraire des Corps imperiaux des ponts et chaussées et des mines.
- [16] Løland, G., 1991. *Current Forces on and Flow Through Fish Farms*. Doktor ingeniøravhandling: Norges Tekniske Høgskole. Division of Marine Hydrodynamics, the Norwegian Institute of Technology.
- [17] Endresen, P. C., Føre, M., Fredheim, A., Kristiansen, D., and Enerhaug, B., 2013. "Numerical modeling of wake effect on aquaculture nets". In ASME 2013 32nd International Conference on Ocean, Offshore and Arctic Engineering, American Society of Mechanical Engineers, pp. V003T05A027–V003T05A027.
- [18] Berstad, A. J., 2012. Verification and benchmarking of aquasim, a software tool for simulation of flexible offshore facilities exposed to environmental and operational loads. report no. 2012-1755-1. Tech. rep., Aquastructures AS. www.aquastructures.no.
- [19] Berstad, A. J., Tronstad, H., and Ytterland, A., 2004. "Design rules for marine fish farms in Norway. calculation of the structural response of such flexible structures to verify structural integrity". In Proceedings of OMAE2004 23rd International Conference on Offshore Mechanics and Arctic Engineering, no. OMAE2004-51577.
- [20] Aquastructures, 2003. Havari laksefjord. Report no. 2003-132.
- [21] Aquastructures, 2005. Teknisk vurdering av anlegg, tustna kommune. Report no. HR-300083-103.
- [22] Berstad, A. J., and Tronstad, H., 2008. "Use of hydroelastic analysis for verification of towed equipment for acquisition of seismic data". In Proceedings of OMAE2008 27th International Conference on Offshore Mechanics and Arctic Engineering, no. OMAE2008-57850.
- [23] Berstad, A. J., and Tronstad, H., 2007. "Development and design verification of a floating tidal power unit". In Proceedings of OMAE2007 26th International Conference on Offshore Mechanics and Arctic Engineering, no. OMAE2007-29052.
- [24] Nygaard, I., 2013. Merdforsøk. kapasitets-tester. report no. 580367.00.01 / mt58 Å13-129. Tech. rep., MARINTEK, Marintek Postboks 4125 Valentinlyst 7450 Trondheim.

Appendix 1

This appendix gives an overview of the parameters used in the numerical model. It is stated how these are derived. Three tables are presented: One for the floater, one for the net and one for mooring system. All input parameters from the model experiment have been scaled to full scale values.

In all column named "Test" shows input parameters from the experiment. The column named "Analysis" shows parameters implemented in AquaSim.

As seen in Tab. 3-5 33 out of 75 parameters used in the numerical analysis has been reported by [24]. The rest of the parameters have been estimated.

As an example, consider the floating tube as seen in Fig. 4(b). This has been scaled to obtain a target EI. The corresponding structural cross sectional area, A or EA has not been reported. The A value used in the analysis has been found by using the A for a full scale polyethylene tube with the same diameter and I as the model experiment. As seen from Fig. 4(b) though, it is evident that the tested tube does not look like a normal tube scaled. The tested tube has the structural capacity in the centre and buoyancy elements clamped to it.

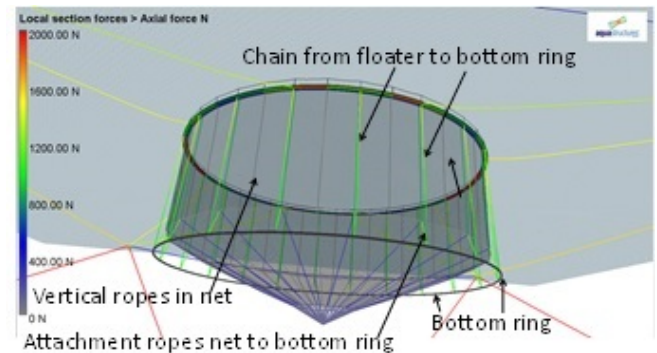


FIGURE 24. STRUCTURAL DESIGN OF NET

Two expressions for the solidity is used. For a knotless mesh the solidity can be expressed as:

$$S_n = \frac{2d}{L} - \frac{d^2}{L^2} \quad (12)$$

Where d is the diameter of the twine and L is the half mesh width. Another definition is:

$$S_{n2D} = \frac{2d}{L} \quad (13)$$

Equation 13 is often denoted the "2D solidity" since it basically is based on summing diameters in both directions.

Table 5 shows data for the mooring system (see also Fig. 4(a)). The mooring system contains bridles to the cage. Buoys are attached to the corner of the frame. All mooring lines, apart from the two mooring lines situated upstream consist of 105 meter rope, and 30 meter chain at the bottom. The two mooring lines situated upstream (denoted ML1 and ML2 in Fig. 5 also consist of spring in order to soften the line stiffness.

There is a lot of measuring equipment in the model experiment (load cells, cables etc.) which may influence the results. The magnitude of such equipment is not reported.

TABLE 3. PARAMETERS FLOATER

Floater	Test	Analysis
Tubes		
No. tubes	2	2
Circumference inner tube [m]	157	157
Diameter inner ring (centre) [m]	50	50
Diameter outer ring (centre) [m]	50.9	50.9
Distance between tubes (c-c) [m]	0.9	0.9
Tube diameter [mm]	450	450
A [m^2]		3.46E-02
EI [N/m^2]	7.72E-04	7.81E-04
E modulus [N/m^2]		9.00E+08
Mass density [kg/m^3]		953
Clamps		
No. clamps	40	40
E modulus [N/m^2]		8.00E+08
I about vertical axis [m^4]		5.878E-06
I about horizontal axis [m^4]		2.50E-04
A [mm^2]		16100
Mass density [kg/m^3]		959
Vertical poles at clamps		
E [N/m^2]		8.00E+08
I in both directions [m^4]		2.01E-06
A [m^2]		5.02E-03
Mass density [kg/m^3]		959.00
Hand railing		
E modulus [N/m^2]		2.44E+09
I in both directions		0
A cross section [mm^2]		24.375
Mass density [kg/m^3]		910

TABLE 4. PARAMETERS OF THE NET STRUCTURE

Net	Test	Analysis
Net mesh		
Diameter [m]	50	50
Depth of vertical net [m]	15	15
Depth to bottom [m]	25	25
Half mesh length [mm]		14.3
Diameter twine [mm]		2.00
Solidity knotless, S_n (Eqn. 12)	26.0%	26.0%
Solidity, S_{n2D} (Eqn. 13)		28.0%
E-modulus [MPa]		1.00E+03
Vertical ropes in net [#]	40	40
Diameter vertical ropes [mm]		19
E-modulus [MPa]		2100
Attachment ropes net to bottom ring [#]		20
Diameter ropes to bottom ring [mm]		19
E-modulus [N/m^2]		2.10E11
Weight centre bottom		
Weight in water [kg]	200	200
Bottom ring		
Diameter, centre [m]		51.8
Outer diameter tube [mm]		280
Depth bottom ring [m]		17
E-modulus [N/m^2]	1.20E+11	1.20E+11
EI [Nm^2]	2.00E+05	2.00E+05
A [m^2]		0.0204
Mass density [kg/m^3]		4321.00
Weight in water [kg/m]	25	25
Chain from floater to bottom ring		
No. of chains [#]	20	20
Leg diameter chain [mm]		16
Weight in air [kg/m]		3.48
E modulus [N/m^2]		1.10E+11

TABLE 5. DATA FOR THE MOORING SYSTEM

Moorings system	Test	Analysis
Bridle		
Bridles at each corner [#]	2	2
Position on cage bridle 1 [Deg]	18	18
Position on cage bridle 2 [Deg]	63	63
Rope length outer part [m]		40
Chain length to floater [m]		8-10
Rope diameter [mm]		48
E-modulus [N/m^2]		2.44E+10
Leg diameter chain [mm]		19
E-modulus [N/m^2]		1.10E+11
Frame		
Length frame both ways [m]	100	100
Depth of frame [m]		7
Rope diameter [mm]		56
E-modulus [N/m^2]		2.44E+10
EA [N]		6.01E+07
Moorings lines		
Length, horizontal, line 3-8 [m]	105	105
Length, horizontal, line 1-2 [m]	100	100
Length of spring in line 1 and 2 [m]	5	5
Length of chain at bottom end [m]	30	30
Depth bottom [m]	52	52
Diameter rope [mm]		56
EA [N]	6.01E+07	6.01E+07
Moorings lines with springs [#]	2	2
Spring stiffness, line 1 and 2 [kN]	137	137
Buoys and couplings below buoys		
Buoys (1 at each corner) [#]	4	4
Buoyancy [kg]	4335	4335
Steel parts for couplings [#]	4	4
Submerged weight of each coupling [kg]	55	55